

**$\psi'$  Polarization due to color-octet quarkonia production**

Adam K. Leibovich

*Lauritsen Laboratory**California Institute of Technology**Pasadena, CA 91125*

(December 2, 2024)

**Abstract**

We calculated the polarization of  $\psi'$  due to  $gg \rightarrow Q\bar{Q}[{}^3P_J^{(8)}]g \rightarrow \psi^{(\lambda)}$  color-octet quarkonia production. We find that at low transverse momenta the  $\psi'$  is unpolarized due to the contributions proportional to the  $L = S = 0$  and  $L = S = 1$  color-octet matrix elements. As  $p_\perp$  increases, the  $\psi'$  mesons become 100% polarized, as predicted by fragmentation calculations. Observation of prompt  $\psi'$  polarization at the Tevatron with this qualitative shape would provide evidence for the color-octet production mechanism.

The study of quarkonia production has recently received renewed attention due to new data and interesting theoretical developments. Traditionally, quarkonia production has been calculated in the color-singlet model (CSM), where the heavy quark-antiquark pair is produced in a color-singlet configuration at distance scales short compared to  $\Lambda_{QCD}$ . While the CSM is successful in describing many phenomenological aspects of quarkonia, it has become clear that it fails to provide a consistent picture of quarkonia production. Order of magnitude discrepancies have been found between CSM predictions and new measurements of  $\psi$  and  $\Upsilon$  production at several colliders. These disagreements have called into question the validity of the CSM, and stimulated new ideas regarding quarkonia production.

Quarkonia are inherently nonrelativistic due to the large mass  $M_Q$  of the heavy quark and antiquark. Consequently, the physics of quarkonia involves a new small parameter, the velocity  $v$  of the heavy constituents inside the  $Q\bar{Q}$  bound state. An effective field theory called Nonrelativistic Quantum Chromodynamics (NRQCD) has been established [1], based on a double power series expansion in the strong interaction fine structure constant  $\alpha_s = g_s^2/4\pi$  and the velocity  $v \sim 1/\log M_Q$ . NRQCD allows for the creation at short distances of a heavy quark-antiquark pair in a color-octet configuration which later hadronized into a colorless final state quarkonia. Similar to Heavy Quark Effective Theory, NRQCD incorporates an approximate spin symmetry, which constrains various multiplet structures, transition rates, and polarizations. There have been many applications of NRQCD to quarkonia production in various high energy processes [2], but the validity of the picture still has to be verified.

NRQCD makes definite predictions of the polarization of  $\psi$ 's produced in a high energy collision. Thus, one test of the color-octet picture would be observing the polarization of  $\psi$  mesons produced at the Tevatron consistent with NRQCD calculations. At large transverse momenta, quarkonia are primarily produced by gluon fragmentation [3–8]. The gluon is nearly real and transverse in the high  $p_\perp$  limit, and the resulting  $Q\bar{Q}[^3S_1^{(8)}]$  pair inherits this spin alignment. The long distance hadronization into a colorless  $\psi$  preserves all angular momentum information, due to the NRQCD approximate spin symmetry. Thus,  $\psi$  mesons produced at large  $p_\perp$  are 100% transversely aligned [9]. Higher order  $\alpha_s$  correction to the

polarization of  $\psi$  from gluon fragmentation have been calculated, and occur at the few percent level [10].

Gluon fragmentation is, however, only valid in the  $p_\perp \gg M_Q$  limit. At low transverse momentum, large numbers of  $\psi$ 's are produced via color-octet states with  $L = S = 0$  and  $L = S = 1$  [11,12]. Corrections to the fragmentation limit are not constrained to preserve the polarization of the  $\psi$ . Therefore, to use quarkonia polarization as a test of the color-octet mechanism, we need to investigate the spin alignment due to these states. In this paper, we will only consider the polarization of  $\psi'$  mesons. A similar analysis for other charmonia and bottomonia states is possible, but these mesons are complicated by feeddown from higher level states.

In the NRQCD formalism, the production cross section for a quarkonia state  $H$  in the reaction  $A + B \rightarrow H + X$  can be written as

$$\sigma(AB \rightarrow HX) = \sum_{ab} \int_0^1 dx_1 dx_2 f_{a/A}(x_1) f_{b/B}(x_2) \hat{\sigma}(ab \rightarrow H), \quad (1a)$$

$$\hat{\sigma}(ab \rightarrow H) = \sum_n C_n^{ab} \langle \mathcal{O}_n^H \rangle. \quad (1b)$$

The sum in (1a) is over all partons in the colliding hadrons, and the parton distribution functions are denoted by  $f_{a/A}$  and  $f_{b/B}$ . The short distance coefficients  $C_n^{ab}$  describe the production of a quark-antiquark in a state  $n$  and can be calculated perturbatively in  $\alpha_s$ . The NRQCD matrix elements  $\langle \mathcal{O}_n^H \rangle$  parameterizes the hadronization of state  $n$  into the quarkonium state  $H$  plus light hadrons [1]. These NRQCD matrix elements contain all the nonperturbative information in the production process, and must be extracted experimentally. The order in the velocity expansion at which each of these matrix elements participates in the  $\psi_Q$  creation processes is governed by simple NRQCD counting rules [13].

The unpolarized cross sections for producing  $\psi'$  mesons in quark-antiquark, quark-gluon, and gluon-gluon scattering have been previously calculated up to  $\mathcal{O}(\alpha_s^3 v^7)$  [11,12]. At this order, the matrix elements that appear in Eq. (1b) are  $\langle \mathcal{O}_1^{\psi'}(^3S_1) \rangle$ ,  $\langle \mathcal{O}_8^{\psi'}(^3S_1) \rangle$ ,  $\langle \mathcal{O}_8^{\psi'}(^1S_0) \rangle$ , and  $\langle \mathcal{O}_8^{\psi'}(^3P_0) \rangle$ . The values of the color-octet matrix elements were extracted in [12] by fitting the magnitudes of the calculated NRQCD cross section to Tevatron data, and are

$$\langle \mathcal{O}_8^{\psi'}(^3S_1) \rangle = (4.6 \pm 1.0) \times 10^{-3} \text{GeV}^3, \quad (2a)$$

$$\frac{\langle \mathcal{O}_8^{\psi'}(^3P_0) \rangle}{M_c^2} + \frac{\langle \mathcal{O}_8^{\psi'}(^1S_0) \rangle}{3} = (5.9 \pm 1.9) \times 10^{-3} \text{GeV}^3. \quad (2b)$$

Only the linear combination of  $\langle \mathcal{O}_8^{\psi'}(^1S_0) \rangle$  and  $\langle \mathcal{O}_8^{\psi'}(^3P_0) \rangle$  could be extracted. The error bars are statistical and do not reflect the potentially large systematic uncertainties in heavy quark masses, color-singlet wavefunctions, parton distribution functions and next-to-leading order corrections. Color-singlet quarkonia production is suppressed relative to the color-octet production, as can be seen in Fig. 5 of Ref. [12], and will be neglected in the following analysis of the polarization.

It is possible to use the results of Ref. [11,12] to obtain the polarization of the final state  $\psi'$  when the intermediate  $Q\bar{Q}$  pair is in a  $^1S_0^{(8)}$  or  $^3S_1^{(8)}$  state. For the intermediate  $^3P_J^{(8)}$  state, however, the analysis in Ref. [12] cannot be used to obtain a polarized cross section. As pointed out in Ref. [10], since heavy quark spin symmetry is an approximate symmetry in the NRQCD Lagrangian,  $L_z$  and  $S_z$  are good quantum numbers. Therefore, to calculate the polarization of the final state  $\psi'$  correctly, we must project the hard scattering amplitude onto states with definite  $L_z$  and  $S_z$ , square the amplitude, and then do the sum over  $L_z$ . A formalism was developed later to correctly calculate the polarization in the NRQCD framework [14]. In Ref. [12], the hard scattering amplitude was projected onto states with definite  $JJ_z$  and then squared. This will give the correct unpolarized cross section [15,14], but will not be useful in calculating the polarized cross section.

Phenomenologically, the contribution to the total cross section from the quark-antiquark and quark-gluon scattering into an intermediate color-octet state with  $L = S = 1$  at the Tevatron is small. The ratio,

$$R = \frac{d\sigma_{gg}(p\bar{p} \rightarrow Q\bar{Q}[^3P_J^{(8)}] \rightarrow \psi')/dp_\perp}{d\sigma(p\bar{p} \rightarrow \psi')/dp_\perp}, \quad (3)$$

is plotted in Fig. 1, where  $d\sigma_{gg}/dp_\perp$  means only gluons were included in the sum in Eq. (1a). In the same figure, the ratio of differential cross sections due to quark-antiquark and quark-

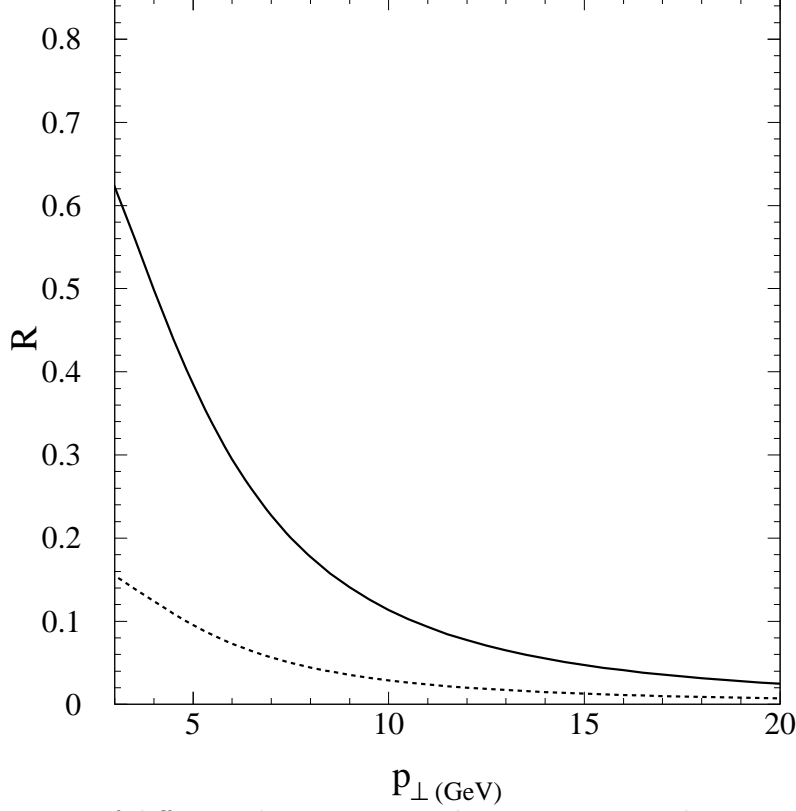


FIG. 1. The ratio  $R$  of differential cross section due to an intermediate  $L = S = 1$  color-octet state over the total differential cross section vs  $p_{\perp}$ . The solid curve illustrates gluon-gluon scattering into the  ${}^3P_J^{(8)}$  state over the total differential cross section. The dashed curve illustrates the ratio of differential cross sections due to quark-antiquark and quark-gluon scattering to the total differential cross section. For both curves,  $\langle \mathcal{O}_8^{\psi'}({}^1S_0) \rangle$  is set to zero.

gluon scattering over the total is also shown.<sup>1</sup> We assumed in this plot that  $\langle \mathcal{O}_8^{\psi'}({}^1S_0) \rangle = 0$ , so that we could assign a value to the  $\langle \mathcal{O}_8^{\psi'}({}^3P_0) \rangle$  matrix element from the linear combination (2b). Since the calculation cannot be trusted for  $p_{\perp} \lesssim 3\text{GeV}$  due to collinear divergences which should be factored into incident parton distribution functions [11], we do not extend the range of the transverse momentum below  $p_{\perp} < 3\text{GeV}$ .

As can be seen in Fig. 1, while gluon-gluon scattering has a sizable contribution to the

---

<sup>1</sup>In this paper, MRSD0 parton distribution functions evaluated at the renormalization scale  $\mu = \sqrt{p_{\perp}^2 + 4M_c^2}$  were used, with  $M_c = 1.48\text{ GeV}$ . A pseudorapidity cut of  $|\eta| \leq 0.6$  was imposed.

total differential cross section, quark-antiquark and quark-gluon scattering contributes less than 20%. Uncertainties in the values of the NRQCD matrix elements, as well as higher order  $\alpha_s$  and  $v$  corrections, will result in larger errors than simply neglecting quark-antiquark and quark-gluon scattering. Within the theoretical accuracy, we can ignore the contribution to the polarization due to  $gq \rightarrow Q\bar{Q}[{}^3P_J^{(8)}]q \rightarrow \psi'^{(\lambda)}$  and  $q\bar{q} \rightarrow Q\bar{Q}[{}^3P_J^{(8)}]g \rightarrow \psi'^{(\lambda)}$ . Therefore, we calculated the cross section  $gg \rightarrow Q\bar{Q}[{}^3P_J^{(8)}]g \rightarrow \psi'^{(\lambda)}$  and combined this with the results from Ref. [12] to obtain the total polarized cross section.

The methods used in calculating the amplitudes are similar to those described in Ref. [12], and the discussion will not be repeated here. The only difference being that we projected the amplitude onto states of definite  $L_z$  and  $S_z$ , squared, and then summed over  $L_z$ . The differential cross sections are shown in the Appendix. If we sum over helicities, we recover the unpolarized cross section from Ref. [12].

The ratio of longitudinal differential cross section to the unpolarized differential cross section,

$$\xi = \frac{\sigma_L}{\sigma_T + \sigma_L}, \quad (4)$$

can be measured in  $\psi' \rightarrow \ell^+\ell^-$  decay. The leptons are distributed in angle according to

$$\frac{d\Gamma(\psi' \rightarrow \ell^+\ell^-)}{d\cos\theta} \propto 1 + \alpha \cos^2\theta, \quad (5)$$

where

$$\alpha = \frac{1 - 3\xi}{1 + \xi}, \quad (6)$$

and  $\theta$  denotes the angle between the lepton momentum in the  $\psi'$  rest frame and the  $\psi'$  momentum in the lab frame. In Fig. 2, we plot  $\alpha$  for prompt  $\psi'$  production at the Tevatron. Since there is only a value for the linear combination in Eq. (2b), we cannot give a definite prediction for  $\alpha$ . Instead, the solid curve represents  $\alpha$  when  $\langle \mathcal{O}_8^{\psi'}({}^3P_0) \rangle = 0$ . The dashed curve illustrates  $\alpha$  when the contribution from  $\langle \mathcal{O}_8^{\psi'}({}^1S_0) \rangle$  is set to zero. The shaded region illustrates the effect of the uncertainties in the matrix elements in Eq. (2).

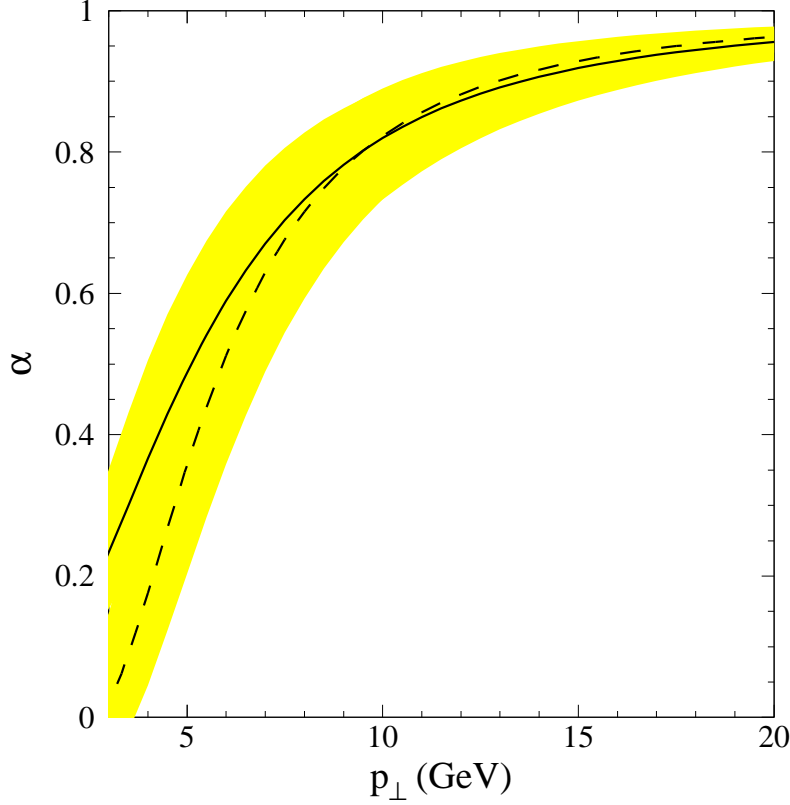


FIG. 2. Coefficient  $\alpha$  which governs the lepton angular distribution in  $\psi' \rightarrow \ell^+ \ell^-$  decay plotted as a function of  $p_\perp$ . The solid and dashed curves illustrate  $\alpha$  for  $\psi'$  production at the Tevatron when  $\langle \mathcal{O}_8^{\psi'}(^3P_0) \rangle$  and  $\langle \mathcal{O}_8^{\psi'}(^1S_0) \rangle$  respectively vanish. The shaded region shows the effect of the uncertainty in the extraction of the matrix elements.

The angular distribution approaches the transverse form  $1 + \cos^2 \theta$  at high  $p_\perp$  as predicted by gluon fragmentation computations [9]. At low transverse momentum, the  $\psi'$  is essentially unpolarized due to  $L = S = 0$  and  $L = S = 1$  color-octet states. Since the two curves are similar in shape, the true value for the angular coefficient should be close to the curves shown. The effect of uncertainties in the matrix elements and higher order corrections can be qualitatively described by slight displacements of the curves in Fig. 2, without changing the asymptotic behaviors. Observation of prompt  $\psi'$  polarization at the Tevatron consistent with the prediction presented in Fig. 2 would give strong support to the color-octet production mechanism.

## **ACKNOWLEDGMENTS**

We wish to thank M. Wise and P. Cho for useful discussions. The work of A.K.L. was supported in part by the U.S. Department of Energy under Grant No. DE-FG03-92-ER40701.



## APPENDIX:

$gg \rightarrow Q\bar{Q}[{}^3P_J^{(8)}]g \rightarrow \psi$  polarized differential cross section:<sup>2</sup>

$$\begin{aligned}
\frac{d\hat{\sigma}^{(\lambda=0)}}{d\hat{t}} &= \frac{5\pi^2\alpha_s^3}{\hat{s}^2 M^3} \langle \mathcal{O}_8^{\psi'}({}^3P_0) \rangle \\
&\times \left\{ \hat{s}^3 \hat{z}^4 (\hat{s}^2 - \hat{z}^2)^4 + M^2 \hat{s}^2 \hat{z}^2 (\hat{s}^2 - \hat{z}^2)^2 (6\hat{s}^6 - 23\hat{s}^4 \hat{z}^2 + 3\hat{s}^2 \hat{z}^4 - 7\hat{z}^6) \right. \\
&\quad + M^4 \hat{s} (\hat{s}^{12} - 34\hat{s}^{10} \hat{z}^2 + 119\hat{s}^8 \hat{z}^4 - 117\hat{s}^6 \hat{z}^6 + 57\hat{s}^4 \hat{z}^8 - 17\hat{s}^2 \hat{z}^{10} + 7\hat{z}^{12}) \\
&\quad - M^6 (7\hat{s}^{12} - 97\hat{s}^{10} \hat{z}^2 + 225\hat{s}^8 \hat{z}^4 - 183\hat{s}^6 \hat{z}^6 + 109\hat{s}^4 \hat{z}^8 - 61\hat{s}^2 \hat{z}^{10} + \hat{z}^{12}) \\
&\quad + M^8 \hat{s} (23\hat{s}^{10} - 183\hat{s}^8 \hat{z}^2 + 328\hat{s}^6 \hat{z}^4 - 291\hat{s}^4 \hat{z}^6 + 164\hat{s}^2 \hat{z}^8 - 11\hat{z}^{10}) \quad (\text{A1a}) \\
&\quad - M^{10} (47\hat{s}^{10} - 248\hat{s}^8 \hat{z}^2 + 366\hat{s}^6 \hat{z}^4 - 255\hat{s}^4 \hat{z}^6 + 58\hat{s}^2 \hat{z}^8 - 2\hat{z}^{10}) \\
&\quad + M^{12} \hat{s} (66\hat{s}^8 - 244\hat{s}^6 \hat{z}^2 + 270\hat{s}^4 \hat{z}^4 - 117\hat{s}^2 \hat{z}^6 + 9\hat{z}^8) \\
&\quad - M^{14} (66\hat{s}^8 - 168\hat{s}^6 \hat{z}^2 + 118\hat{s}^4 \hat{z}^4 - 23\hat{s}^2 \hat{z}^6 + \hat{z}^8) \\
&\quad + M^{16} \hat{s} (47\hat{s}^6 - 76\hat{s}^4 \hat{z}^2 + 30\hat{s}^2 \hat{z}^4 - 3\hat{z}^6) - M^{18} \hat{s}^2 (23\hat{s}^4 - 21\hat{s}^2 \hat{z}^2 + 4\hat{z}^4) \\
&\quad \left. + M^{20} \hat{s}^3 (7\hat{s}^2 - 3\hat{z}^2) - M^{22} \hat{s}^4 \right\} / \left[ \hat{s} \hat{z}^2 (\hat{s} - M^2)^5 (\hat{s} M^2 + \hat{z}^2)^4 \right],
\end{aligned}$$

$$\begin{aligned}
\sum_{|\lambda|=1} \frac{d\hat{\sigma}^{(\lambda)}}{d\hat{t}} &= \frac{5\pi^2\alpha_s^3}{\hat{s}^2 M^3} \langle \mathcal{O}_8^{\psi'}({}^3P_0) \rangle \\
&\times \left\{ 2\hat{s}^3 \hat{z}^4 (\hat{s}^2 - \hat{z}^2)^4 + 2M^2 \hat{s}^2 \hat{z}^2 (\hat{s}^2 - \hat{z}^2)^2 (2\hat{s}^6 - 11\hat{s}^4 \hat{z}^2 + 3\hat{s}^2 \hat{z}^4 - 3\hat{z}^6) \right. \\
&\quad + M^4 \hat{s} (6\hat{s}^{12} - 68\hat{s}^{10} \hat{z}^2 + 226\hat{s}^8 \hat{z}^4 - 258\hat{s}^6 \hat{z}^6 + 147\hat{s}^4 \hat{z}^8 - 58\hat{s}^2 \hat{z}^{10} + 10\hat{z}^{12}) \\
&\quad - M^6 (42\hat{s}^{12} - 318\hat{s}^{10} \hat{z}^2 + 722\hat{s}^8 \hat{z}^4 - 619\hat{s}^6 \hat{z}^6 + 272\hat{s}^4 \hat{z}^8 - 46\hat{s}^2 \hat{z}^{10} + 6\hat{z}^{12}) \\
&\quad + M^8 \hat{s} (138\hat{s}^{10} - 782\hat{s}^8 \hat{z}^2 + 1311\hat{s}^6 \hat{z}^4 - 854\hat{s}^4 \hat{z}^6 + 264\hat{s}^2 \hat{z}^8 - 58\hat{z}^{10}) \quad (\text{A1b}) \\
&\quad - M^{10} (282\hat{s}^{10} - 1223\hat{s}^8 \hat{z}^2 + 1550\hat{s}^6 \hat{z}^4 - 784\hat{s}^4 \hat{z}^6 + 206\hat{s}^2 \hat{z}^8 - 12\hat{z}^{10}) \\
&\quad + M^{12} \hat{s} (396\hat{s}^8 - 1308\hat{s}^6 \hat{z}^2 + 1240\hat{s}^4 \hat{z}^4 - 450\hat{s}^2 \hat{z}^6 + 69\hat{z}^8) \\
&\quad - M^{14} (396\hat{s}^8 - 970\hat{s}^6 \hat{z}^2 + 642\hat{s}^4 \hat{z}^4 - 147\hat{s}^2 \hat{z}^6 + 6\hat{z}^8) \\
&\quad + 3M^{16} \hat{s} (94\hat{s}^6 - 160\hat{s}^4 \hat{z}^2 + 63\hat{s}^2 \hat{z}^4 - 6\hat{z}^6) - 3M^{18} \hat{s}^2 (46\hat{s}^4 - 47\hat{s}^2 \hat{z}^2 + 8\hat{z}^4) \\
&\quad \left. + 6M^{20} \hat{s}^3 (7\hat{s}^2 - 3\hat{z}^2) - 6M^{22} \hat{s}^4 \right\} / \left[ \hat{s} \hat{z}^2 (\hat{s} - M^2)^5 (\hat{s} M^2 + \hat{z}^2)^4 \right].
\end{aligned}$$

---

<sup>2</sup>The differential cross sections are expressed in terms of the variables  $\hat{s}$ ,  $\hat{z} \equiv \sqrt{\hat{t}\hat{u}}$  and  $M \equiv 2M_Q$ .

## REFERENCES

- [1] G. T. Bodwin, E. Braaten and G. P. Lepage, Phys. Rev. D **51**, 1125 (1995).
- [2] See E. Braaten, S. Fleming and T. C. Yuan, Ohio State preprint OHSTPY-HEP-T-96-001 (hep-ph/9602374), to be published in *Annual Review of Nuclear and Particle Science*, and references therein.
- [3] E. Braaten and T. C. Yuan, Phys. Rev. Lett. **71**, 1673 (1993).
- [4] E. Braaten and T. C. Yuan, Phys. Rev. D **50**, 3176 (1994).
- [5] E. Braaten, M. A. Doncheski, S. Fleming and M. L. Mangano, Phys. Lett. **B333**, 548 (1994).
- [6] D. P. Roy and K. Sridhar, Phys. Lett. **B339**, 141 (1994).
- [7] M. Cacciari and M. Greco, Phys. Rev. Lett. **73**, 1586 (1994).
- [8] E. Braaten and S. Fleming, Phys. Rev. Lett. **74**, 3327 (1995).
- [9] P. Cho and M. Wise, Phys. Lett. **B346**, 129 (1995).
- [10] M. Beneke and I. Z. Rothstein, Phys. Lett. **B372**, 157 (1996).
- [11] P. Cho and A. K. Leibovich, Phys. Rev. D **53**, 150 (1996).
- [12] P. Cho and A. K. Leibovich, Phys. Rev. D **53**, 6203 (1996).
- [13] G. P. Lepage, L. Magnea, C. Nakhleh, U. Magnea and K. Hornbostel, Phys. Rev. D **46**, (1992) 4052.
- [14] E. Braaten and Y.-Q. Chen, Phys. Rev. D **54**, 3216 (1996).
- [15] M. Beneke and I. Z. Rothstein, Phys. Rev. D **54**, 2005 (1996).